Numerical Simulations of Mechanochemical Responses for Confined PBXs under Low-velocity Impact

Kun Yang[a], Yanqing Wu[a*], Fenglei Huang[a], Zhu Zhang[b]
a State Key Laboratory Explosion Science and Technology, Beijing Institute of Technology, Beijing 100081, China
b School of Applied Science, Taiyuan University of Science and Technology, Taiyuan 030024, China

1 Abstract

A series of two-dimensional mechanical-chemical simulations were performed to describe the different reaction stages of confined PBX charge undergoing low-velocity impact (~100m/s). The ratio of length to diameter of the samples are 0.5, 1.0, and 2.0, respectively. An ignition criterion of effective plastic work was employed to predict the ignition response of the PBX charge. A pressure-dependent reaction rate equation was utilized to describe slow burning and its growth to deflagration following ignition. Simulated results show that the incident stress wave reflection from lateral surfaces contributed to the formation of potential ignition regions for cylinder-shaped charges with a length-to-diameter ratio of 2.0. After the ignition, the reaction violence characterized by the reaction rate of the mass fraction increased as impact velocity increased for 150–400m/s, whereas impact velocity had little influence on the reaction violence for 80–150m/s.

2 Introduction

Numerous abnormal impact scenarios may cause accidental initiation of energetic materials. Significant focus on the safety of energetic materials is required to ensure that these materials can be transported or stored safely until they are utilized exactly as intended [1].

The variations of impact velocity have influences on ignition response and reaction violence of the PBX charge. Most previous studies have investigated the shock initiation of explosives (SDT) [2-4]. In shock initiation, the strength (1–2 GPa and higher) and the duration (~0.1 μs) of initial shock waves are sufficient to induce detonation rapidly. In practice, explosives are more likely to be subjected to low pressure impact loading conditions, where XDT (unknown to detonation) often occurs. For the low-velocity impact, the impact pressure is relatively low (~0.1 GPa), and its duration is relatively long (~1 ms); hence, a two-stage compression wave (elastic and plastic wave) is formed. Chemical reaction first occurs at the local regions of charge rather than throughout the entire regions. The violence of the reaction induced by such mild

*Correspondence to: wuyqing@bit.edu.cn (Yanqing WU)

impacts is uncertain, including the non-reaction event, possible ignition, steady burning, or even a violent explosion. Such non-shock impact ignitions have been studied by several researchers and are still the subject of continuing research [5-9].

In the present work, a numerical framework describing the behavior of deformation, ignition, burning or deflagration, and temperature information efficiently for confined HEs undergoing low-velocity impact are developed. The three main objectives are as follows: (i) to investigate the relation between mechanical response and ignition of PBXs under different impact velocities; (ii) to compare the differences of ignition events of the charge with three different ratios of length to diameter; (iii) to predict the violence of chemical reaction inside the confined charge under different impact velocities.

3 Model Descriptions

An elastoplastic constitutive relation was employed to describe the dynamic response of PBXs and to improve the practicability of the model in a finite element framework. The strength model was pressure- and strain-rate-dependent. Moreover, the effects of temperature and chemical reaction process on the yield strength were also considered. The strength model can be described as,

$$\sigma_Y = (1-\lambda)(C_1 + C_2 \cdot p)(1 + C_3 \ln \dot{\varepsilon}^*)\left[1-(T^*)^{C_4}\right] \tag{1}$$

$$T^* = \frac{T - T_0}{T_m - T_0} \tag{2}$$

where C_1-C_4 denote the strength of PBXs under quasi-static load, the hardening coefficient of material under pressure, the coefficient of strain rate, and the coefficient of temperature, respectively; p and λ denote pressure and mass fraction reaction; $\dot{\varepsilon}^* = \dot{\varepsilon}/\dot{\varepsilon}_0$ is the equivalent plastic strain-rate normalized to $\dot{\varepsilon}_0$ =1.0 s^{-1}; and T^* is the dimensionless temperature calculated by Eq. (2), where T is the absolute temperature, T_0 is the room temperature, and T_m is the melting temperature.

The deposition of sufficient thermal energy in a finite volume of explosive strongly influences ignition. Ma et al. [10] assumed that the heat deposition results from the effective plastic work. The plastic work is effective for depositing thermal energy only when the specific plastic power (P_{st}) increases to a critical value (P_0). The ignition occurs when the effective plastic work (W_{st}) reaches a threshold value (W_0). The dual ignition criterion is expressed as,

$$P_{st}(t) = \sigma_m(t) \cdot \dot{\varepsilon}_{pl}(t) \ge P_0 \tag{3}$$

$$W_{st}(t) = \int_{t_1}^{t} P_{st}(t)\,dt \ ; \ W_0 = W_{st}(t_{ig}) \tag{4}$$

where P_{st} (t) and W_{st} (t) denote a function of the specific plastic power and the effective specific plastic work, respectively, with time t; P_0 and W_0 are ignition threshold parameters [10]; σ_m is von-Mises stress; $\dot{\varepsilon}_{pl}$ is the effective plastic strain rate; and t_1, t_{ig} denote the time when the plastic work begins to be deposited and the ignition occurs, respectively.

A reaction kinetics equation and two equations of state were employed based on the concept of reactive flow first proposed by Lee [3] to describe the chemical reaction process of HEs. In this simulation, a pressure-dependent reaction rate was selected to describe slow burning and deflagration of explosives. The reaction kinetics equation can be described as follows:

$$\frac{d\lambda}{dt} = G(1-\lambda)^a \lambda^b p^c \tag{5}$$

where λ is the mass fraction reaction and a, b, c, and G are constants.

The Grüneisen and JWL equations of state were utilized to describe the pressure-volume relation for reactants and gaseous products, respectively. Following the analysis of Handley [11], the equation of state with an isentrope as the reference curve has analytic expressions for temperature. Two temperature calculation formulations were therefore imported to simulate the thermal response of HEs undergoing chemical reaction. In the present study, unreacted explosive and gaseous products are assumed to be in thermomechanical equilibrium in a reacted element.

4 Results and Discussion

The experimental geometry of the target assembly is shown in Fig. 1(a). A cylindrical PBX charge with three different sizes: Φ40×78mm, Φ40×40mm, and Φ40×20mm (see Fig. 1(b)) was confined by a 45-mm-thick steel back plate and a 15-mm-thick steel sleeve. A 5-mm-thick Teflon retaining ring positioned the charge within the confinement. The steel projectile impacted normally on the front surface of the charge. Only half of the structural geometry model was established using the 2D finite element numerical model, as shown in Fig. 1(c). Four locations within the sample labeled by location #1–4 were selected to describe the following analysis efficiently. The initial distances from the impact surface of locations #1–4 are 0, 26, 52, and 78 mm, respectively. Simulations were performed with Drexh-2D, a two-dimensional explicit code of Lagrangian finite element.

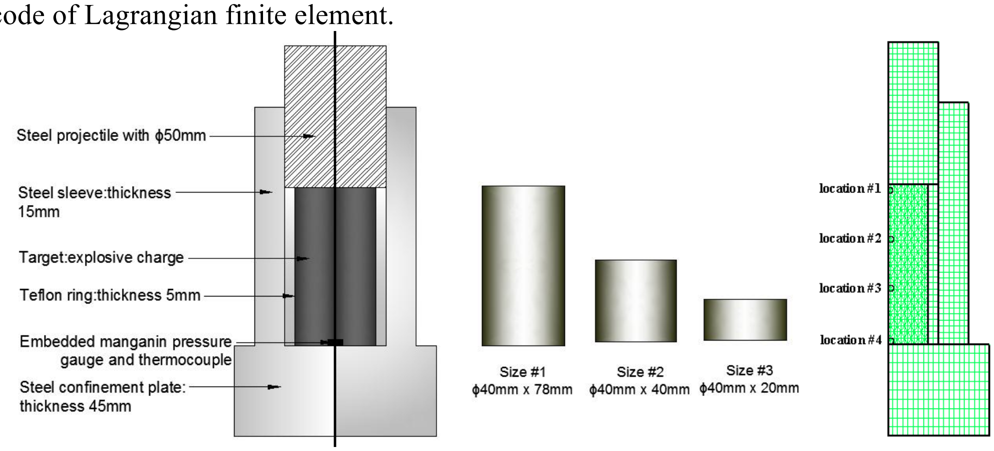

Figure 1. (a) The experimental geometry model (b) The PBX charge with three different sizes (c) 2D finite element numerical model of the target assembly

4.1 The evolution of the stress under different impact velocities

Figure 2(a) presents the pressure histories at location #4 (charge size #1) with impact velocities of 100, 120, 150, and 180 m/s. In the selected region, a plastic wave (traveling at the plastic sound velocity) propagates following an elastic wave (traveling at longitudinal sound velocity). At the impact velocity of 180 m/s, the plastic region was not observed in the curve because the loading strength was high enough to form a shockwave. The propagation velocity of the shockwave was much higher than that of a plastic wave. As the impact velocity decreased to 100 m/s, a 54-μs-duration pressure plateau appeared within 35–89 μs due to the relatively low propagation velocity of the plastic wave. Following the pressure plateau, the appearance of rapid growth should be related to the occurrence of ignition because a more violent reaction followed by ignition can produce a large-scale pressure increment in a short time.

The evolution of the stress profile along the axis line of the charge (size #1) at impact velocity of 120 m/s is plotted in Fig. 2(b). The incident wave front propagated through the charge with 0.3 GPa during 0–30 μs. The pressure plateau covers regions that have undergone plastic deformation. The deposition of the effective plastic work was sufficiently large to ignite the charge at location #1 after a 40 μs-duration. After 30 μs, the total stress at the back surface comprises the stress of incident and reflected waves. The charge at location #4 was ignited at 50 μs. The pressure curve appeared a peak at 20 mm, which results from the influence of incident stress wave reflection from the lateral surfaces. If the accumulation of the heat energy at the pressure peak is sufficiently large, the charge may be ignited at this location.

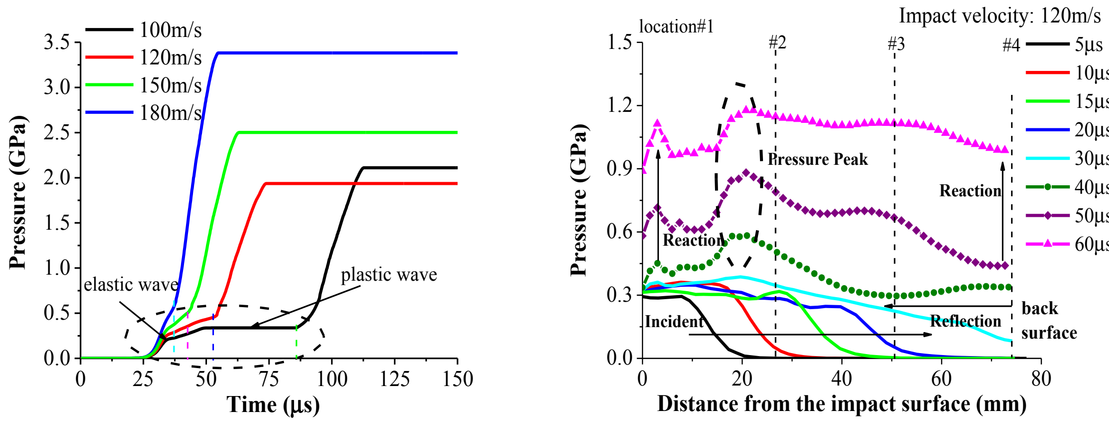

Figure 2. (a) The pressure histories at location #4 with 100, 120, 150, and 180 m/s impact velocities. (b) The pressure versus position curves at various times for charge with size #1 at 120m/s.

4.2 Prediction of ignition event for PBX charge with different sizes

Figure 3(a) presents the mass fraction reaction contour of the charge (size #1) at an impact velocity 100 m/s, in which three potential ignition regions (#1, #2, and #3) are marked. Regions #1 and #2 are located at the corner of the impact surface, where the maximum of the mass fraction reaction is approximately 6%. The occurrence of ignition at these regions results from the level of stress concentrations at these sites being much higher than average values. In region #3 (20 to 35 mm distance from the impact surface), the ignition is triggered due to the effect of the overlapping of the incident and lateral reflected stress waves at the axis line of the charge. Unlike 100 m/s, at an impact velocity of 180 m/s, the entire charge reaction at the impact surface was caused, as presented in Fig. 3(b). This phenomenon indicates the strength of incident shock wave is high enough (0.5 GPa) to cause the entire charge react.

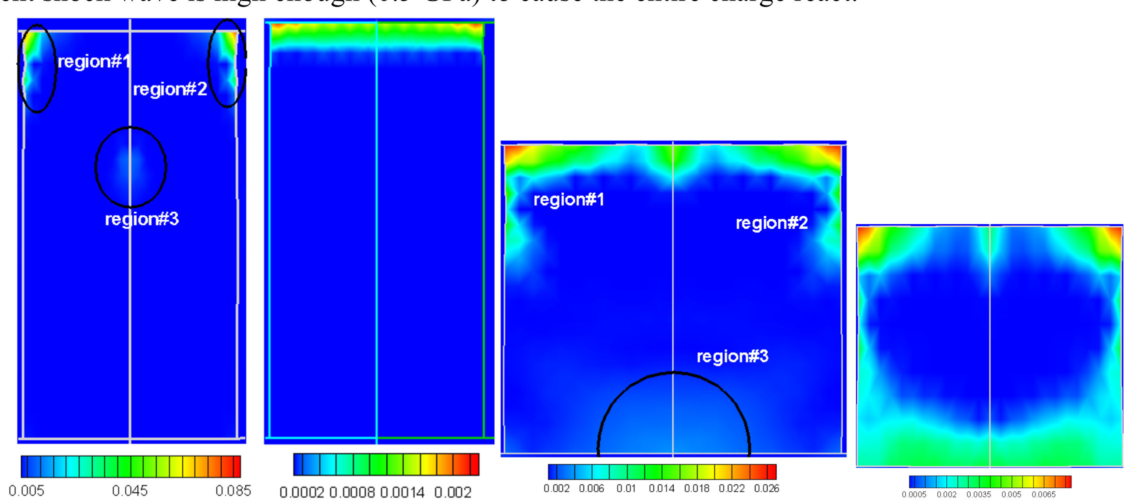

Figure 3. Mass fraction reaction contour of PBX sample (a) Size #1, impact velocity: 100 m/s, t=50 μs; (b) Size #1, impact velocity: 180 m/s, t=6 μs; (c) Size #2, impact velocity: 120 m/s, t=20 μs (d) Size #3, impact velocity: 120 m/s, t=12 μs.

Figures 3(c) and 3(d) show ignition regions of the charge with size #2 and size #3, respectively. For the charge with size #2, region #3 was formed due to the overlapping of the incident and reflected stress waves at the back surface. If the length-to-diameter ratio of the charge is small enough (e.g. size #3: 0.5), the incident wave will propagate with a short duration between the impact surface and back surface. Ignition regions at impact and back surfaces combined with each other. The ignition front therefore gradually converged from the boundary to the center of the charge, as shown in Fig. 3(d).

4.3 Prediction of reaction violence under different impact velocities

Figures 4(a) and 4(b) present the reaction rate of mass fraction histories at the back surface with a series of impact velocities for sizes #1 and #2. In Fig. 4(a), when the impact velocity is higher than 120m/s (150, 180, and 210 m/s), the maximum of reaction rate at an impact velocity of 210 m/s is 24.7% higher than the value at an impact velocity of 150 m/s. In addition, at an impact velocity of 210 m/s, the duration of the chemical reaction is 8.9 μs lower than that of 150 m/s. The above analysis indicates that the release rate of chemical energy at 210 m/s is much higher than that at 150 m/s. In other words, reaction violence increases with the increasing impact velocity. For 80, 100, and 120 m/s impact velocity, the maximum of reaction rate at an impact velocity of 120 m/s is only 8.5% higher than the value at an impact velocity of 80 m/s. Meanwhile, the duration of a chemical reaction between 80 m/s and 120 m/s has little difference.

The ignition front at medium-level impact velocity (>120m/s) follows the propagation of the initial incident shock wave. The strength of shockwave is sufficiently high to induce a deflagration after ignition. The violence of deflagration increases with the increasing strength of shock wave. For the low-level impact (≤120m/s), the low-strength incident stress wave can only cause chemical reactions at local regions, as discussed in Fig. 3(a). Following the ignition, steady burning is triggered inside the charge. Thus, impact velocity has little effect on the reaction violence for the low-level impact.

As shown in Fig. 4(b), impact velocity has little influence on reaction violence of the charge with size #2 at the back surface. The length of the charge with size #2 is sufficiently small that reflected waves formed at the back surface can propagate to the impact surface in 15-μs-duration. When the steady burning is triggered inside the charge under the low-level impact, reflected waves will accelerate the rate of chemical reaction, thereby catching the reaction rate induced by medium-level impact. In addition, the maximum of reaction rate of the charge with size #2 under medium-level impact (e.g. 210 m/s) was smaller than that of size #1. That's because the overlapping of the incident waves and reflected waves formed in lateral surfaces increased the reaction violence in size #1.

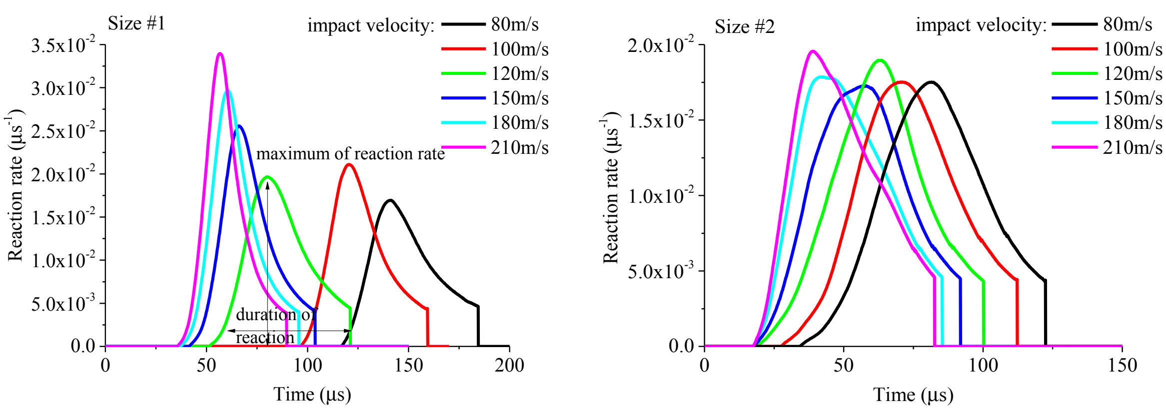

Figure 4(a) and (b). The predicted reaction rate of mass fraction histories with size #1 and #2 at 80, 100, 120, 150, 180, and 210 m/s impact velocities.

5 Conclusions

Using hydrodynamic-code, Drexh-2D, a series of two-dimensional mechanical-chemical simulations was performed to describe the reaction stages of confined PBX charge undergoing low-velocity impact (~100m/s). Simulated results show that the incident stress wave reflection from lateral surfaces contributed to the formation of potential ignition regions for charges with a length-to-diameter ratio of 2.0. After the ignition, the reaction violence characterized by the reaction rate of the mass fraction increased as impact velocity increased for 150–400m/s, whereas impact velocity had little influence on the reaction violence for 80–150m/s. This phenomenon results from the deflagration induced in the higher-velocity impact, and its violence is related to the strength of the shock wave. However, the lower-velocity stress wave only induces ignition at local regions, and sequent burning is no longer sensitive to the strength of the incident wave.

In future work, a damage sub-model, which includes the creation of porosity and cracks, should be incorporated in the reactive model because the evolution of damage will increase the specific surface area and accelerate the burning process.

Acknowledgments

The authors would like to thank the Chinese National Nature Science Foundation (Grant Nos. 11572045) and Science Challenge Project (JCKY2016212A501) and Opening fund from Safety ammunition research and Development Center (RMC2015B03) and Shanxi Province Science Foundation for Youths (2015021021) for supporting this project.

References

[1] Tarver CM, Chidester SK. (2005). On the violence of high explosive reactions. J. Pres. Vessel. Technol. 127: 39-45.
[2] Campbell AW, Davis WC, Ramsay JB, Travis JR. (1961). Shock initiation of solid explosives. Phys. Fluids. 4: 511-521.
[3] Lee EL, Tarver CM. (1980). Phenomenological model of shock initiation in heterogeneous explosives. Phys. Fluids. 23: 2362-2372.
[4] Tarver CM, Chidester SK, Nichols AL. (1996). Critical conditions for impact-and shock-induced hot spots in solid explosives. J. Phys. Chem. 100: 5794–5799.
[5] Chidester SK, Green LG, Lee CG. (1993). A frictional work predictive method for the initiation of solid high explosives from low pressure impacts. Proc. 10th International Detonation. 785–792.
[6] Idar DJ, Lucht RA, Straight JW, et al. (1998). PBX 9501 high explosive violent reaction experiments. Proc. 11th International Detonation. 101–110.
[7] Scammon RJ, Browning RV, Middleditch J, Dienes JK, Haverman KS, Bennett JG. (1998). Low amplitude project: structural analysis and prediction of low order reaction. Proc. 11th International Detonation. 111–118.
[8] Gruau C, Picart D, Belmas R, et al. (2009). Ignition of a confined high explosive under low velocity impact, Int. J. Imp. Eng. 36: 537-550.
[9] Reaugh JE, Jones AG. (2010). Mechanical damage, ignition, and burn: experiment, model development, and computer simulations to study high-explosive violent response (HEVR). Proc. 14th International Detonation.
[10] Ma DZ, Chen PW, Zhou Q, Dai KD. (2013). Ignition criterion and safety prediction of explosives under low velocity impact. J. Appl. Phys. 114: 1-5.
[11] Handley CA. Numerical modeling of two HMX-based plastic-bonded explosives at the mesoscale.

University of St Andrews. 2011.